THE RELATIONSHIP BETWEEN PERC TIME AND FIELD-SATURATED HYDRAULIC CONDUCTIVITY FOR CYLINDRICAL TEST HOLES

W.D. Reynolds[1], K. Galloway[2], and D.E. Radcliffe[3]

Abstract

Correlations between Perc Time (PT) and field-saturated hydraulic conductivity (K_{fs}) are often used in development of on-site water recycling and treatment facilities that operate by infiltration into unsaturated soil. The accuracy and utility of these correlations is suspect, however, because they differ greatly from each other, and they derive from empirical regressions or simplified analyses that incompletely describe the factors affecting PT and K_{fs}. An accurate and physically based analytical expression relating PT to K_{fs} for cylindrical test holes was used to compare and assess six PT versus K_{fs} correlations. Some of the correlations appear to apply only for specific test conditions, while others are of unknown origin, or seem inconsistent with established soil water flow theory. It was consequently recommended that the proposed analytical expression relating PT to K_{fs} be used in place of the existing PT versus K_{fs} correlations, as it provides PT-K_{fs} results that are functionally linked, founded on rigorous infiltration theory, and based on known and well-defined borehole test conditions.

Introduction

Percolation (Perc) Time, PT [T L^{-1}], is defined as the time period, Δt [T], required for the water level in an open, unlined pit or borehole in unsaturated soil to fall a specified distance, ΔH [L] (e.g. Division of Environmental Quality, 2007; NebGuide, 2011). The PT value is determined via the "Percolation Test" (Division of Environmental Quality, 2007); and for decades, PT has been the soil permeability indicator used in development of on-site absorption fields, such as subsurface wastewater infiltration (septic) drainfield systems (SWIS), subsurface drip irrigation (SDI) systems, storm water infiltration galleries, and various other decentralized water recycling and treatment facilities that operate by infiltrating water through soil (e.g. Division of Environmental Quality, 2007; NebGuide, 2011; Toronto and Region Conservation Authority, 2012). It has been understood for some time, however, that PT is less than ideal because it is not just a function of soil permeability, but also a function of test conditions; i.e. the PT value can change substantially with pit/borehole dimensions, depth of water ponding, soil capillary properties, and background soil moisture content at the time of the test (e.g. Elrick and Reynolds, 1986; Fritton et al., 1986). The PT indicator nonetheless continues to be widely used because PT criteria remain in the design specifications and regulatory codes of many types of absorption

[1]Greenhouse and Processing Crops Research Centre, Agriculture and Agri-Food Canada, Harrow, Ontario, Canada N0R 1G0. dan.reynolds@agr.gc.ca

[2]President, Dynamic Monitors (a business unit of Engineering Technologies Canada Ltd.), 1-16 Myrtle St, Stratford, PEI Canada C1B 2W2. kelly@dynamicmonitors.com

[3]Crop and Soil Sciences Department, University of Georgia, Athens GA, USA 30602. dradclif@uga.edu

fields (e.g. NebGuide, 2011; Toronto and Region Conservation Authority, 2012; Penn State Extension, 2014).

Tyler (2001) presented a procedure to estimate wastewater infiltration and hydraulic linear loading rates based on soil characteristics (ie. soil consistence, texture, structure) rather than PT. In that paper, Tyler states that "all characteristics used while determining loading rates are collected by a soil scientist". This "soil morphology" approach is replacing an exclusively PT based approach in many US onsite sewage guidelines. This is the preferred approach of manufacturers of subsurface drip irrigation (SDI) equipment (eg. Geoflow 2015 and Netafim, 2015). Ruskin (2015, personal communication, Galloway) expressed the opinion that "for larger systems, Geoflow feels more confident in a soils analysis over a measured percolation rate which can be affected by recent rainfall events, etc." Current Netafim design guidelines also recommend determining SDI loading rates on the basis of soil morphology. Their guide (Netafim, 2015) states "While some perc rate data using the mpi method (minutes per inch) has been created, it is not generally considered an accurate way to determine hydraulic loading rate since the claims are not backed by scientific soil science studies."

Radcliffe (2015, personal communication, Galloway) notes that even where a soil morphology approach is preferred, PTs are sometimes conducted if the soil is marginal and the site assessor wants to justify that it is suitable. A two-pronged approach is used by the British Columbia Ministry of Health (2014). Soil loading rates (hydraulic loading rate and linear loading rate) are selected on the basis of soil morphology ***and*** PT or Kfs; the lower of the two is used for final design/sizing. British Columbia uses the same conservative approach for both conventional septic drainfields and SDI systems.

The most logical alternative to PT is the “field-saturated” hydraulic conductivity, K_{fs} [L T^{-1}], which measures the permeability of “field-saturated” soil, wherein the pore space contains entrapped or encapsulated air as well as water under positive pressure (Elrick and Reynolds, 1986). This parameter is largely independent of test conditions, and it is directly applicable to many absorption field applications (e.g. land-based effluent disperal systems, storm water infiltration galleries) because ponded infiltration into unsaturated soil typically produces field-saturated zones adjacent to the infiltration surfaces (Elrick and Reynolds, 1986). Unfortunately, K_{fs} criteria are still absent from most design specifications and regulatory codes governing absorption fields, although some exceptions now exist for onsite wastewater treatment systems (e.g. Canadian Standards Association, 2012).

Ksat tests are sometimes required for the design of large scale (ie. non-residential) onsite wastewater treatment systems. Ksat or Kfs values are used for various hydraulic analyses including groundwater or effluent mounding analysis and lateral flow analysis (eg. North Carolina Department of Health and Human Services, 2014 and Canadian Standards Association, 2012).

Hence, application of K_{fs} from design and regulatory perspectives requires that it be accurately and functionally linked to the existing PT criteria in most absorption field codes and technical guidelines.

Past attempts to develop PT versus K_{fs} relationships using statistical regressions (e.g. Winneberger, 1974; Jabro, 2009) and approximate analytical solutions (Amoozegar, 1997; Fritton et al., 1986) have met with limited success (as evidenced by excessive data scatter, see e.g. Fig. 1 in Fritton et al., 1986; Figs. 1-3 in Jabro, 2009) because the functional relationships and interactions among PT, K_{fs}, and borehole/pit test conditions were incompletely described. However, an accurate and physically based analytical expression relating PT to K_{fs} for cylindrical test holes has been proposed (Reynolds, 2015) from which usable PT versus K_{fs} relationships are now possible. Hence, the objectives of this report were to: i) present an accurate and physically based PT versus K_{fs} relationship; ii) characterize the response of this relationship to variation in borehole test conditions; iii) compare this relationship to some others currently used in the development of absorption fields; and iv) suggest how the physically based PT versus K_{fs} relationship might be applied in absorption field development.

Analysis

The physically based PT versus K_{fs} expression in Reynolds (2015) for cylindrical test holes in unsaturated soil can be simplified to:

$$PT = \frac{\Delta t}{\Delta H} = \frac{\overline{C}a^2}{K_{fs}\left[2\overline{H}^2 + \overline{C}a^2 + \left(2\overline{H}/\alpha^*\right)\right]} \tag{1}$$

where a [L] is test hole radius, $\overline{H}$ [L] is average water level (ponding depth) in the test hole over time interval, Δt [T], α^* [L^{-1}] is soil sorptive number for ponded infiltration, and $\overline{C}$ [-] is a "shape function". From a physical perspective, the first term in the right-hand denominator of Eq. (1) represents infiltration from the test hole due to the hydrostatic pressure of the ponded water, the second term represents gravity-driven infiltration out through the base of the test hole, and the third term represents infiltration due to the capillary suction or "capillarity" of the surrounding unsaturated soil. The shape function may be expressed as (Reynolds, 2008; Zhang et al., 1998):

$$\overline{C} = \left[\frac{\left(\overline{H}/a\right)}{Z_1 + Z_2\left(\overline{H}/a\right)}\right]^{Z_3} \tag{2}$$

where Z_1, Z_2 and Z_3 are dimensionless empirical constants which depend somewhat on soil texture, structure and sorptive number, α^* (Table 1). Relationships similar to Eq. (1) appear in Elrick and Reynolds (1986) (their Eq. 6) and in Radcliffe and West (2000) (their Eqs. 5 and 6), but with somewhat different shape functions.

It should also be noted that Eq. (1) applies only after an initial constant head "presoak" period is conducted to establish steady, field-saturated infiltration in the soil adjacent to the test hole (Reynolds, 2015; Elrick and Reynolds, 1986). As described by Reynolds (2008) and elsewhere, users of the CHWP method can conclude that steady state conditions have been achieved when the flow rate into the soil is approximately constant over several successive observations. For users of the Guelph Permeameter (Soilmoisture Equipment Corporation) or ETC Pask Permeameter (Dynamic Monitors), this involves obtaining a relatively constant rate of fall on the

permeameter reservoir for a minimum of three to five successive readings. Elrick et al (1989) provided estimates for the time to reach steady state based on unpublished theoretical data and field experience. They estimated times "on the order of 30 minutes or fewer for permeable soils ($K_{fs} > 10^{-5} ms^{-1}$), and up to several hours in slowly permeable soils ($K_{fs} < 10^{-7} ms^{-1}$)".

It is important to note that the presoak period to achieve steady state flow is not the same as the presoak period prescribed by some codes and regulatory guides to allow time for smectitic clays to swell. The length of time required for this "swelling clay presoak period" seems somewhat arbitrary as it varies considerably from one jurisdiction or country to another. According to Reynolds (2015), it typically is in the range of 2 hours to 30 hours.

The soil sorptive number (α^*) can be expanded to:

$$\alpha^* = \frac{\alpha}{[1 - \exp(\alpha\psi_a)]} \tag{3}$$

where ψ_a [L] is the antecedent or background pore water pressure head in the soil surrounding the test hole, and α [L^{-1}] may be viewed as the "integrally correct" slope of the soil's unsaturated hydraulic conductivity versus pore water pressure head relationship, $K(\psi)$ (Reynolds and Elrick, 1987). Since pore water pressure head determines water content via the soil water characteristic curve (Hillel, 1998), then ψ_a determines the background moisture content of the soil surrounding the test hole. Note also that since α is related to α^* via Eq. (3), then the slope of the $K(\psi)$ relationship (i.e. α) is determined to a large extent by the soil's texture and structure (Table 1).

As mentioned in Reynolds (2008, 2015) and elsewhere, α^* is approximately equal to α in Eq. (3) when the soil is at about field capacity or drier (i.e. $\psi_a \leq -1$ m) because the $\exp(\alpha\psi_a)$ term in Eq. (3) is near zero under those conditions. This fortunate situation, combined with the correlation among soil texture-structure classification, soil capillarity category and α^* (Table 1), forms the basis of the Single-Head CHWP analysis (Reynolds, 2008).

Substituting Eq. (3) into (1) produces:

$$PT = \frac{\Delta t}{\Delta H} = \frac{\overline{C}a^2}{K_{fs}\left[2\overline{H}^2 + \overline{C}a^2 + \frac{2\overline{H}[1 - \exp(\alpha\psi_a)]}{\alpha}\right]} \tag{4.1}$$

which can be simplified to:

$$PT = mK_{fs}^{-1} \tag{4.2}$$

or

$$K_{fs} = mPT^{-1} \tag{4.3}$$

where

$$m = \frac{\overline{C}a^2}{\left[2\overline{H}^2 + \overline{C}a^2 + \frac{2\overline{H}\left[1-\exp(\alpha\psi_a)\right]}{\alpha}\right]} \quad ; 0 < m < 1 \qquad (4.4)$$

For a cylindrical test hole, Eq. (4.1-4.4) delineates the primary functional relationships among PT, K_{fs} and test hole conditions, where the test conditions (represented by Eq. 4.4) incorporate a flow geometry component (a, $\overline{H}$), a soil texture-structure component (α), and an antecedent soil moisture component (ψ_a).

Equations (4.1-4.4) can be applied from either a Constant Head Well Permeameter (CHWP) perspective, or a Percolation Test (Perc Test) perspective. In the CHWP approach, K_{fs} is measured using one of the standard CHWP methodologies (e.g. Reynolds, 2008), and the corresponding PT is then calculated via Eqs. (4.2) and (4.4). In the Perc Test approach, PT is determined by measuring the fall in borehole water level, ΔH, during time interval, Δt (cf. Eq. 4.1), and the corresponding K_{fs} is then calculated via Eqs. (4.3) and (4.4). Hence, Eqs. (4.1-4.4) can be used to determine PT from K_{fs}, or K_{fs} from PT. It should be noted, however, that Eq. (4.2) yields an "equivalent" PT value since borehole water level is held constant during a CHWP measurement (i.e. ΔH = 0); while K_{fs} determined via Eq. (4.3) applies for the average borehole water level ($\overline{H}$) over the measured ΔH interval (Reynolds, 2015; Radcliffe and West, 2000).

Characteristics of Equations (4.1)-(4.4)

Since the K_{fs} of natural porous media typically varies over orders of magnitude (e.g. Warrick and Nielsen, 1980), Eqs. (4.2) and (4.3) are often best presented in logarithmic form or plotted using logarithmic axes. The logarithmic (base 10) form of Eq. (4.2) is:

$$\log_{10}(PT) = -\log_{10}(K_{fs}) + \log_{10}(m) \qquad (5)$$

Equation (5) (or Eq. 4.2 plotted on logarithmic axes) indicates that $\log_{10}(PT)$ versus $\log_{10}(K_{fs})$ is linear with slope = -1 and intercept = $\log_{10}(m)$, provided that m is constant over the plotted K_{fs} range. Hence, the slope of $\log_{10}(PT)$ vs. $\log_{10}(K_{fs})$ (or the K_{fs} exponent in Eq. 4.2) is -1 regardless of the test condition values (i.e. $\overline{H}$, a, α or ψ_a), provided that the test condition values remain constant. However, if test condition values are not constant over the K_{fs} range, then $\log_{10}(PT)$ vs. $\log_{10}(K_{fs})$ will not be linear. Figure 1 demonstrates the effect of constant test conditions, where it is seen that the slope of $\log_{10}(PT)$ vs. $\log_{10}(K_{fs})$ (or the K_{fs} exponent in Eq. 4.2) remains fixed at -1, while the PT-axis intercept (or m value in Eq. 4.2) increases with

Table 1. Texture-structure classifications with corresponding capillarity category, representative sorptive number, α^*, and Z-constants in Eq. (2) (adapted from Reynolds and Lewis, 2012). The soil capillarity categories assume that antecedent pore water pressure head, ψ_a, is sufficiently negative to produce near-maximum soil capillarity for that category (Reynolds and Elrick, 1987; Reynolds et al., 1985).

Texture - Structure Classification	Soil Capillarity Category	Representative α^* (m^{-1})	Z_1 (-)	Z_2 (-)	Z_3 (-)
Compacted, structureless, clayey or silty materials such as landfill caps and liners, lacustrine or marine sediments, etc.	Very Strong	≤ 1	2.081	0.121	0.672
Porous materials that are both fine textured and massive; includes unstructured clayey and silty soils, as well as very fine to fine structureless sandy materials.	Strong	4	1.992	0.091	0.683
Most structured and medium textured materials; includes structured clayey and loamy soils, as well as medium single-grain sands. This category is generally the most appropriate for agricultural soils.	Moderate	12[1]	2.074	0.093	0.754
Coarse and gravelly single-grain sands; may also include some highly structured soils with numerous cracks and/or biopores.	Weak	36	2.074	0.093	0.754
Gravels; very coarse sands, etc. containing negligible amounts of coarse/medium/fine/very fine sand, silt and clay; may also include porous media with extensive networks of large macropores.	Negligible	≥ 100	2.074	0.093	0.754

[1]Note that Z_1, Z_2 and Z_3 become effectively constant for moderate to negligible capillarity ($\alpha^* \geq 9$ m^{-1}).

increasing test hole radius (a), α value and ψ_a value, but decreases with increasing average ponding depth ($\overline{H}$). Plot 1 in Figure 2 demonstrates the effect of changing test conditions where $\log_{10}(PT)$ vs. $\log_{10}(K_{fs})$ is curvilinear with slope less steep than -1 because decreasing K_{fs} was accompanied by decreasing test hole radius, decreasing α, increasing average ponding depth and increasing (less negative) ψ_a. Note from Plot 2, however, that if test conditions are made constant by using the average a, α, $\overline{H}$ and ψ_a values from Plot 1, then $\log_{10}(PT)$ vs. $\log_{10}(K_{fs})$ returns to linearity with slope = -1.

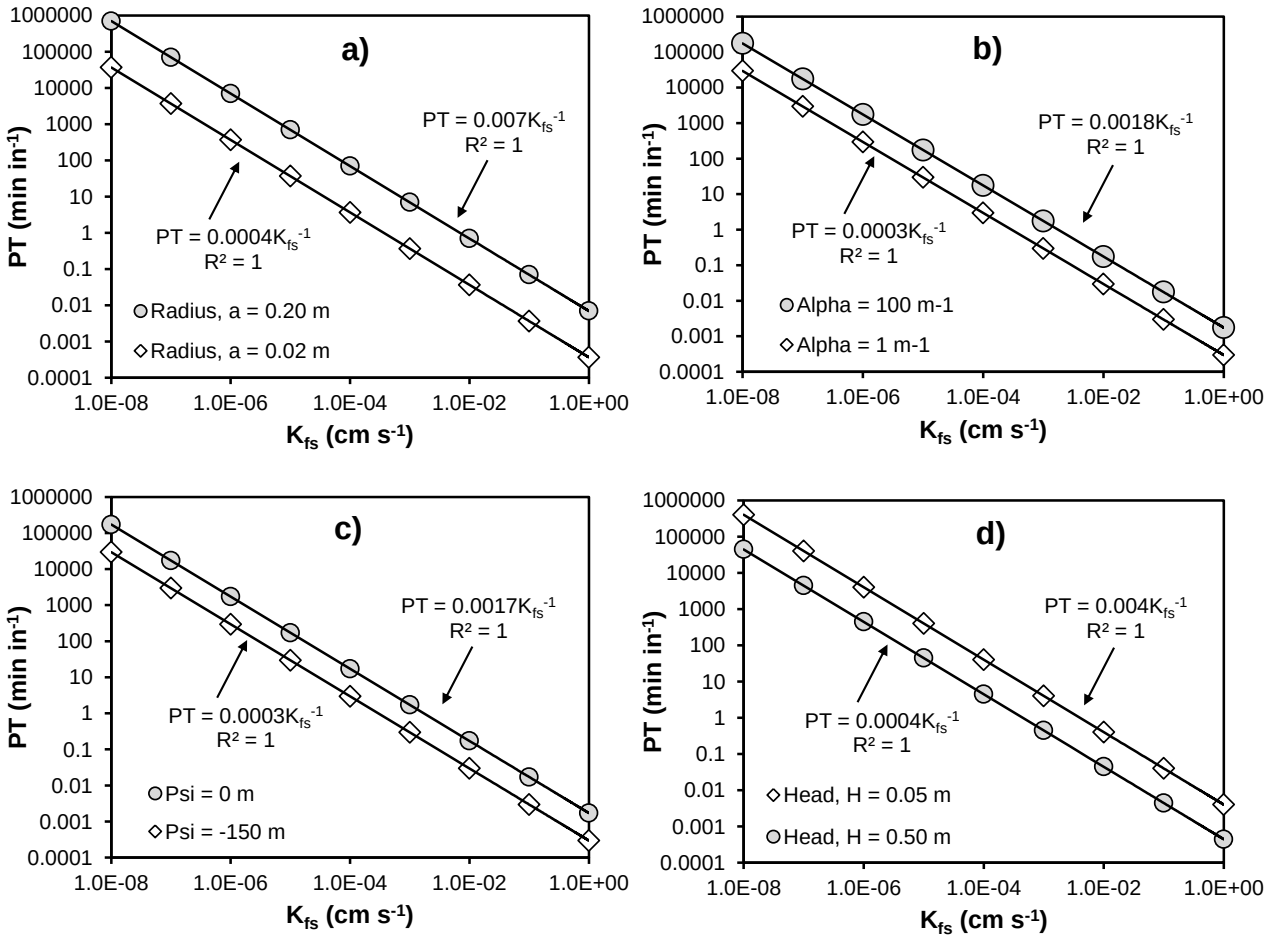

Figure 1. Effect of constant test condition parameters (Eq. 4.4) on Perc Time (PT) versus field-saturated hydraulic conductivity (K_{fs}): a) test hole radius (Radius); b) soil α value (Alpha); c) antecedent soil pore water pressure head (Psi); d) test hole ponding depth (Head). In Fig. 1a: H = 0.20 m, α = 12 m^{-1}, ψ_a = -150 m; Fig. 1b: a = 0.05 m, H = 0.20 m, ψ_a = -150 m; Fig. 1c: a = 0.05 m, H = 0.20 m, α = 1 m^{-1}; Fig. 1d: a = 0.05 m, α = 12 m^{-1}, ψ_a = -150 m.

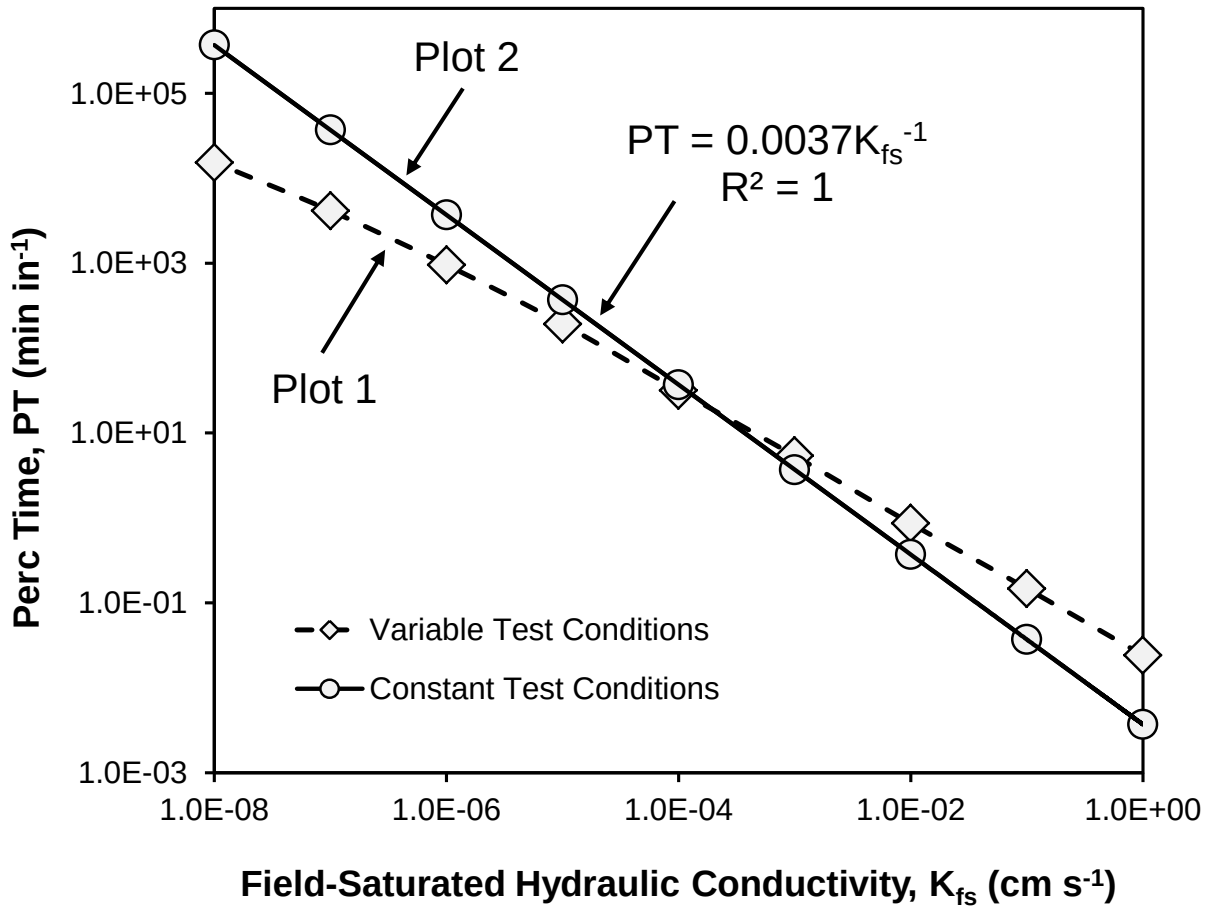

Figure 2. Perc time, PT, versus field-saturated hydraulic conductivity, K_{fs}, for variable test conditions (Plot 1) and constant test conditions (Plot 2) (Eq. 4.1-4.4). For variable test conditions: as K_{fs} decreases from 10^{0} to 10^{-8} cm s^{-1}, test hole radius (a) deceases from 0.20 to 0.04 m, ponded head (H) increases from 0.05 to 0.45 m, α decreases from 100 to 1 m^{-1}, and ψ_a increases from -150 m to -1 m. For constant test conditions: a = 12 cm, H = 0.25 m, α = 32 m^{-1}, ψ_a = -25 m.

Comparison of Equations (4.1-4.4) to Existing PT versus K_{fs} Relationships

Figure 3 compares Eq. (4.2) to six PT versus K_{fs} correlations currently used for developing septic tank leach fields, where the Eq. (4.2) relationship assumes constant test conditions with $\overline{H}$ = 0.15 m, a = 0.10 m, $\psi_a \leq$ -1 m, and $\alpha^* = \alpha$ = 12 m^{-1}. It is seen that three basic patterns emerge: i.e. the Georgia sand, loam and clay correlations which are linear and separate, but parallel to each other and to Eq. (4.2); the Connecticut and Virginia correlations which are non-linear, effectively overlapping each other and Eq. (4.2) for $K_{fs} \leq 3 \times 10^{-4}$ cm s^{-1}, but divergent for $K_{fs} > 3 \times 10^{-4}$ cm s^{-1}; and the Ontario correlation which has a much lower (less negative) slope and cuts across all other relationships. Although the precise origins of the Georgia, Connecticut, Virginia and Ontario correlations are currently obscure, they can nonetheless be interpreted (at least on a cursory level) using the Eq. (4.2) characteristics illustrated in Figures 1 and 2.

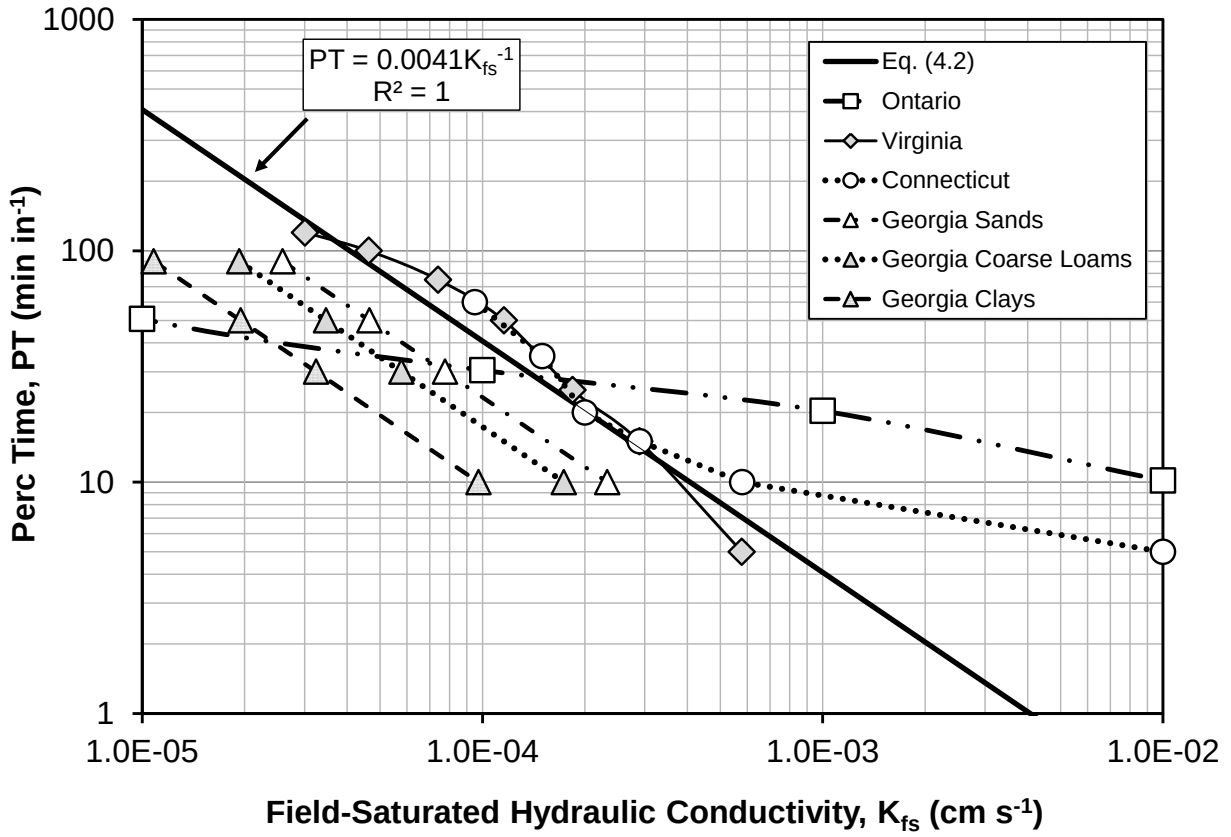

Figure 3. Some existing Perc Time (PT) vs. field-saturated hydraulic conductivity (K_{fs}) correlations (Ontario, Virginia, Connecticut, Georgia sands, Georgia coarse loams, Georgia clays) compared to Eq. (4.2). Constant test conditions were assumed for Eq. (4.2), i.e. H = 0.15 m, a = 0.10 m, $\alpha^* = \alpha = 12$ m^{-1}, $\psi_a = -150$ m.

The Georgia correlations (Fig. 3) are log-linear and parallel to Eq. (4.2) because they were apparently developed using Eq. (5) in Radcliffe and West (2000), which is similar to Eq. (4.3) above for constant test conditions. The correlations apply for $\overline{H}$ = 0.152 m and a = 0.051 m (as specified in the Modified Taft Engineering Center Perc Test), and K_{fs} was calculated for arbitrary PT = 10, 30, 50 and 90 min in^{-1}, with α^* and $\overline{C}$ (Table 1) set for strong soil capillarity (Georgia clays correlation), moderate capillarity (Georgia coarse loams correlation) and weak-negligible capillarity (Georgia sands correlation) (Environmental Protection Division, 2013).

The Virginia, Connecticut and Eq. (4.2) relationships are seen to be roughly coincident for 3×10^{-5} cm s^{-1} $\leq K_{fs} \leq 3 \times 10^{-4}$ cm s^{-1} (Fig 3). The test condition values of $\overline{H}$ = 0.15 m, a = 0.10 m, $\psi_a \leq -1$ m and $\alpha^* = \alpha = 12$ m^{-1} in Eq. (4.2) may consequently be reasonable averages of the actual values used (or implicit) in the Virginia and Connecticut correlations over that K_{fs} range. However, both the non-linearity in the Virginia and Connecticut correlations and their substantial divergence for $K_{fs} > 3 \times 10^{-4}$ cm s^{-1} implies that some or all of the test conditions changed with K_{fs}. The strong divergence might also indicate that non-borehole methods (e.g. soil cores, soil texture correlations) were used to obtain the high-end K_{fs} values. In any case, the accuracy of the

Virginia and Connecticut relationships is suspect, especially for $K_{fs} > 3 \times 10^{-4}$ cm s^{-1}, due to their non-linearity and increasing divergence from Eq. (4.2).

The Ontario PT versus K_{fs} correlation (Fig. 3) appears to be derived from measured PT and "notional estimates" of K_{fs} based on geotechnical soil descriptors, including texture, structure, density, mineralogy, organic content, plasticity and liquid limit (Ontario Ministry of Municipal Affairs and Housing, 1997). Its use of non-borehole methods to obtain K_{fs} likely explains the low slope and non-linearity of the relationship. At any rate, this correlation seems substantially inconsistent with established soil water (borehole) flow theory (Eq. 1), and should probably be used with extreme caution or avoided completely.

Recommendations for Estimating PT from K_{fs} Measurements or Vice Versa

It is clear from Figures 1-3 that test condition effects (i.e. Eq. 4.4) cannot be ignored or simplified when estimating PT from K_{fs} (Eq. 4.2), or when estimating K_{fs} from PT (Eq. 4.3). Furthermore, borehole water level ($\overline{H}$) and radius (a) need to be flexible to help maintain feasible PT measurement times; and it is known that α^*, α and ψ_a often vary with K_{fs} (e.g. Reynolds et al., 1985), which in turn causes $\log_{10}(PT)$ vs. $\log_{10}(K_{fs})$ relationships to be non-linear with average slopes shallower than -1 (e.g. Fig. 2). It is therefore recommended that relationships such as those given in Figure 3 not be used to estimate PT from K_{fs} or vice versa. Instead, PT or K_{fs} should be determined directly from Eq. (4.1-4.4). Briefly, this involves: i) using a constant head well permeameter (CHWP) to maintain a head of water in the test hole at constant ponding depth until steady flow is attained; ii) applying a CHWP method to obtain K_{fs} (Reynolds, 2008) or a Perc Test method to determine PT (Reynolds, 2015); and iii) using Eqs. (4.2) and (4.4) to calculate PT from K_{fs} (if the CHWP test was used), or Eqs. (4.3) and (4.4) to calculate K_{fs} from PT (if the Perc Test was used). Worked examples are given in Appendix A.

Discussion and Concluding Remarks

Equations (4.1)-(4.4) and Figures 1-2 clearly demonstrate that the relationship between PT and K_{fs} is non-unique due to the effects of borehole test condition parameters (i.e. changes in the values of H, a, α and ψ_a). As a result, none of the PT versus K_{fs} correlations in Figure 3 are generally applicable, especially those where K_{fs} is apparently determined using simplified borehole methods or non-borehole methods. The applicability of some correlations could be extended by standardizing borehole ponding depth (H) and radius (a) to specified values, however the flexibility and utility of the CHWP and Perc Test methods would then be somewhat reduced. Site-to-site (or even borehole-to-borehole) variations in soil texture-structure (α) and antecedent pore water pressure head (ψ_a) would need to be factored into the analysis, otherwise, substantial changes in the PT versus K_{fs} correlation could result (cf. Fig. 1b,c). Hence, all of the PT versus K_{fs} correlations in Figure 3 can lead to substantial error if actual borehole test conditions (i.e. values selected for H, a, α and ψ_a) differ from those for which the correlations were derived. It appears that the only way to reliably determine PT from K_{fs} or vice versa is to directly apply Eqs. (4.1)-(4.4) to each borehole measurement using the procedures outlined in Appendix A.

Procedure A1. in the Appendix shows how to determine PT from Kfs using the single-ponded height CHWP method. It is anticipated this procedure will have the most utility for jurisdictions where wastewater absorption field and SDI system sizing is based wholly or in part, on PT. The Single-PT analysis has advantages of increased speed and simplicity (relative to the Dual-PT and Multiple-PT approaches, Reynolds, 2015), but also potential limitations related to subjectivity in site-estimation of the soil sorptive number, α^*). However, as long as the soil moisture condition is less than its field capacity, α^* can be selected from one of five general capillarity categories (via Table 1) which are primarily related to the soil structure and texture. Fortunately, the determination of Kfs is not overly sensitive to the selection of α^* (Elrick et al, 1989). One of the authors (Galloway) has observed that practitioners with basic training in site evaluation and soil classification can usually estimate α^* and not be off by more than two categories (usually only one or none) from the optimal category. As shown by Reynolds (2008), selecting a larger H and borehole radius reduces the effect of error due to poor selection of α^*. Therefore, the accuracy of the single-ponded height method should be sufficient for onsite wastewater and stormwater system design applications, especially when considering typical variations in Kfs and PT for natural soil (e.g. Warrick and Nielsen, 1980).

As mentioned previously, α^* is approximately equal to α in Eq. (3) when the soil is at about field capacity or drier (i.e. $\psi_a \leq$ -1 m) because the $\exp(\alpha\psi_a)$ term in Eq. (3) is near zero under those conditions. It should be kept in mind, however, that the smaller the value of α, the more negative ψ_a has to be in order to cause $\alpha^* = \alpha$; and as a result, ψ_a may have to be much more negative than -1 m for the Single-Head analysis to be accurate in some fine-textured, structureless materials such as compacted heavy clays. Such soils are typically very limiting or even not suitable for the installation of fully in-ground, wastewater absorption fields. Practitioners should be capable of identifying such soils (and assessing their capacity to infiltrate effluent) on the basis of soil morphology alone.

In addition, wet (near-saturated) soils of all types are above field capacity and can have $\alpha^* >> \alpha$ because ψ_a is near zero (cf. Eq. 3), and this may in turn cause the Single-Head CHWP analysis to overestimate K_{fs} in fine-textured, structureless soils that are very wet (Reynolds, 2008, 2015). Practitioners should therefore be capable of recognizing that soil conditions are at or drier than field capacity as a prerequisite to using Table 1 to determine Kfs. One working definition of "field capacity" is the water content that exists in the soil once drainage stops after a soaking (saturating) rain. Cessation of soil drainage corresponds roughly with the time at which tile drains stop flowing after a rain event. As a rough "rule of thumb", soils at field capacity water content or drier do not compress under foot and they tend to crumble (rather than remold or smear) when worked in the hand.

The field capacity soil water content usually corresponds to the pore water pressure head (or matric potential) of ψ = -1 m (some prefer/claim field capacity ψ = -3 m in arid region soils, and ψ = -0.5 m in humid region soils such as the UK); and it is the pore water pressure head that actually imparts soil capillarity, not the soil water content. Field measurement of near-surface ψ using a tensiometer (eg. Quickdraw tensiometer, Soilmoisture Equipment Corp., CA) should be used if practitioners are not confident in their ability to assess the field capacity condition based on judgement alone.

The CHWP method represents an improvement over previous borehole techniques by addressing all three components of borehole flow: 1) flow due to the hydrostatic pressure of the ponded water, 2) gravity-driven infiltration out through the base of the test hole, and 3) infiltration due to the capillary suction or "capillarity" of the surrounding unsaturated soil. The field saturated hydraulic conductivity, Kfs, determined using the CHWP technique, is a much more scientifically and technically sound indicator of soil permeability than the outdated PT. Kfs testing controls for variables that can substantially affect the PT such as pit/borehole dimensions, depth of water ponding, soil capillary properties, and background soil moisture content at the time of the test.

Rather than arbitrary and lengthy pre-soak periods, permeameter users monitor the rate of fall on the permeameter reservoir until several successive readings have been recorded (steady state flow has been achieved). This removes the subjectivity in ensuring the test has run long enough. The enforcement of arbitrary regulatory requirements for presoaking of all well holes during Kfs testing would be unfortunate and completely unnecessary for most soils. Regulators are encouraged to instead develop alternative guidelines (based on soil morphology or other means) for practitioners to identify smectitic swelling clays and to only require prolonged presoaking periods for those soils. This would save many practitioners and homeowners from excessive time and cost burdens. For example, prolonged presoaking could be required for any soil with an "unsoaked" (but steady state) Kfs value $<10^{-7}ms^{-1}$ or having a texture class of Clay Loam or finer.

It is expected that the PT criteria will eventually be replaced with Kfs criteria in the majority of onsite wastewater codes and guidelines. In the meantime, the PT vs. Kfs correlation described in this paper will provide practitioners and regulators with a scientifically defensible means of relating the two.

Literature Cited

Amoozegar, A., 1997. Comparison of saturated hydraulic conductivity and percolation rate: implications for designing septic tank systems, in: Bedinger, M.S., Johnson, A.I., Fleming, J.S. (Eds.), Site Characterization and Design of On-Site Septic Systems. Am. Soc. Testing and Materials, ASTM STP 1324, pp. 129-143.

British Columbia Ministry of Health, Health Protection Branch, 2014. Sewerage System Standard Practice Manual, Version 3, British Columbia, Canada. http://www2.gov.bc.ca/assets/gov/environment/waste-management/sewage/spmv3-24september2014.pdf

Canadian Standards Association, 2012. CSA B65-12 Installation Code for Decentralized Wastewater Systems. Canadian Standards Association, Toronto, ON, Canada.

Division of Environmental Quality, 2007. Percolation Testing Manual. Commonwealth of the Northern Mariana Islands, Gualo Rai, Saipan. 91 pp.

Elrick, D.E., Reynolds, W.D., 1986. An analysis of the percolation test based on three-dimensional saturated-unsaturated flow from a cylindrical test hole. Soil Sci. 142, 308-321.

Elrick, D.E., Reynolds, W.D., K.A.Tan, 1989. Hydraulic conductivity measurements in the unsaturated zone using improved well analyses. Groundwater Monitoring Review, Summer 1989, 184-193.

Environmental Protection Division, 2013. Large Community Subsurface Design Guidance, May 2013, Georgia Environmental Protection Division, USA.

Fritton, D.D., Ratvasky, T.T., Petersen, G.W., 1986. Determination of saturated hydraulic conductivity from soil percolation test results. Soil Sci. Soc. Am. J. 50, 273-276.

Hillel, D., 1998. Environmental Soil Physics. Academic Press, Toronto, ON, Canada.

Jabro, J.D., 2009. Predicting saturated hydraulic conductivity from percolation test results in layered silt loam soils. J. Environ. Health 72, 22-26.

NebGuide, 2011. Residential onsite wastewater treatment: conducting a soil percolation test. Institute of Agriculture and Natural Resources, University of Nebraska-Lincoln Extension, Lincoln, Nebraska, USA, 4 pp.

North Carolina Department of Health and Human Services, Division of Public Health, 2014. Recommended Guidance for In-situ Measurement of Saturated Hydraulic Conductivity by the Constant Head Well Permeameter Method and for Reporting Results, Raleigh, NC, USA.

Ontario Ministry of Municipal Affairs and Housing (OMMAH), 1997. Supplementary Guidelines to the Ontario Building Code 1997. SG-6 Percolation Time and Soil Descriptions. Toronto, ON, Canada.

Penn State Extension, 2014. Site evaluation for on-lot sewage systems (F-163). Penn State Cooperative Extension, Pennsylvania State University, University Park, Pennsylvania, USA, 6 pp.

Radcliffe, D.E., West, L.T., 2000. Relating saturated hydraulic conductivity to percolation and borehole permeameter tests. Soil Survey Horizons 41(4), 99-103.

Reynolds, W.D., 2015. A unified perc test – well permeameter methodology for absorption field investigations. Geoderma (in press).

Reynolds, W.D., 2008. Saturated hydraulic properties: well permeameter, in: Carter, M.R. and Gregorich, E.G. (Eds.), Soil Sampling and Methods of Analysis (2nd ed.). Canadian Society of Soil Science. CRC Press, Boca Raton, FL., USA, pp. 1025-1042.

Reynolds, W.D., Elrick, D.E., 1987. A laboratory and numerical assessment of the Guelph Permeameter method. Soil Science 144, 282-299.

Reynolds, W.D., Lewis, J.K., 2012. A drive point application of the Guelph Permeameter method for coarse-textured soils. Geoderma 187-188, 59-66.

Reynolds, W.D., Elrick, D.E., Clothier, B.E., 1985. The constant head well permeameter: effect of unsaturated flow. Soil Science 139, 172-180.

Ruskin, R, 2015. Personal email communication, Galloway K.

Toronto and Region Conservation Authority, 2012. Low Impact Development, Stormwater Management, and Design Guide, Stormwater Management Criteria, Appendix C: Water Balance and Recharge. Toronto and Region Conservation Authority, Downsview, ON, Canada.

Tyler, E.J. 2001. "Hydraulic Wastewater Loading Rates To Soil." In On-Site Wastewater Treatment, Proc. 9th National Symposium on Individual and Small Community Sewage Systems (11-14 March 2001, Fort Worth, Texas, USA), Ed. K. Mancl., St. Joseph, Mich. ASAE, pp. 80-86.

Warrick, A.W., Nielsen, D.R., 1980. Spatial variability of soil physical properties in the field, in: Hillel, D. (Ed.), Applications of Soil Physics. Academic Press, Toronto, ON, Canada, pp. 319-355.

Winneberger, J.T., 1974. Correlation of three techniques for determining soil permeability. J. Environ. Health 37, 108-118.

Zhang, Z.F., Groenevelt, P.H., Parkin, G.W., 1998. The well-shape factor for the measurement of soil hydraulic properties using the Guelph Permeameter. Soil & Till. Res. 49, 219-221.

Appendix A

A1. Determination of PT from CHWP measurements of K_{fs}

Auger a Constant Head Well Permeameter (CHWP) borehole to the depth of interest using recommended procedures (e.g. Reynolds, 2008). The borehole radius (a) and depth of water ponding (H) should be set to values that wet a soil volume comparable to the sample volume of interest. Essentially, the wetted zone should wet a large enough volume of soil to yield a Kfs value that is representative of the soil.

Presoak the borehole to achieve steady, field-saturated infiltration in the soil adjacent to the borehole by setting constant H on the CHWP, and monitoring CHWP flow rate until it becomes steady. Determine K_{fs} and α^* using the Single-Head (recommended), Dual-Head or Multiple-Head CHWP analysis (Table A1, see also Reynolds, 2008). Use K_{fs}, α^* and Eqs. (3), (4.2) and (4.4) to determine the "equivalent" PT that corresponds to the H, a, α^* and K_{fs} values (Table A1). The calculated PT value is referred to as "equivalent" in this case because borehole water level is held constant (at H) by the CHWP, thereby preventing direct measurement of $PT = \Delta t/\Delta H$ (Eq. 4.1).

Some permeameter manufacturers have developed convenient "quick reference tables" based on formulas A1 and A2 which calculate Kfs and PT based on a range of reservoir rates of fall, and fixed values for the permeameter reservoir size, ponded head (H), auger size (well hole radius) and for the various α^* values. A different set of tables can be easily generated for other H and auger sizes if desired. These tables could be further extended to reflect the newly developed PT and Kfs correlation represented by equation A3.

Table A1. Constant Head Well Permeameter (CHWP) Determination of Field-Saturated Hydraulic Conductivity (K_{fs}) and Equivalent Perc Time (PT) using the Single-Head CHWP Analysis: Example calculations.

CHWP Single-Head Equations (Reynolds, 2008):

$$K_{fs} = \frac{CQ_S}{\left[2\pi H^2 + C\pi a^2 + \left(2\pi H / \alpha^*\right)\right]} \quad \text{(A1)}$$

$$C = \left[\frac{\left(H/a\right)}{Z_1 + Z_2\left(H/a\right)}\right]^{Z_3} \quad \text{(A2)}$$

where Q_S = steady flow rate out of CHWP reservoir ($m^3\ s^{-1}$)
H = steady borehole ponding depth (m)
a = borehole radius (m)
α^* = representative soil sorptive number (m^{-1})

Soil type:	structured loam (determined by visual inspection)
Antecedent soil moisture:	drier than field capacity (i.e. $\psi_a < -1$ m)
Representative soil α*:	12 m^{-1} (Table 1)
C-value Z parameters:	Z_1 = 2.074; Z_2 = 0.093; Z_3 = 0.754 (Table 1)
Set Ponding Depth:	H = 0.15 m
Set Borehole Radius:	a = 0.03 m

Measured steady flow rate out of CHWP reservoir: Q_S = 30 $cm^3\ min^{-1}$ = 5 x 10^{-7} $m^3\ s^{-1}$

C-value (Eq. A2): 1.6669

K_{fs} (Eq. A1): 3.71 x 10^{-6} m s^{-1} = 3.71 x 10^{-4} cm s^{-1} = 0.32 m d^{-1}

Conversion of CHWP K_{fs} to equivalent Perc Time, PT (Eq. 4.2 in text):

$$PT = mK_{fs}^{-1} = \frac{Ca^2}{K_{fs}\left[2H^2 + Ca^2 + \left(2H/\alpha^*\right)\right]} \quad \text{(A3)}$$

PT = 5655.50 s m^{-1} = 0.94 min cm^{-1} = 2.39 min in^{-1}

A2. Determination of K_{fs} from Perc Test measurements of PT

Auger and presoak the Perc Test borehole using the same procedures as in A1 above for the CHWP test. After steady flow at constant ponding depth (H) is attained, stop flow from the CHWP and monitor the decline in H with time (t). Calculate several successive PT values using:

$$PT_1 = \frac{\Delta t_1}{\Delta H_1} = \frac{t_1 - t_0}{H_0 - H_1}; \quad (6.1)$$

$$PT_2 = \frac{\Delta t_2}{\Delta H_2} = \frac{t_2 - t_1}{H_1 - H_2}; \quad (6.2)$$

$$PT_3 = \frac{\Delta t_3}{\Delta H_3} = \frac{t_3 - t_2}{H_2 - H_3}; \quad \text{etc.} \quad (6.3)$$

where $t_0 = 0$ is the start of the falling head phase, H_0 = H at t_0, H_1 = H at t_1, etc. At least two H versus t measurements must be made to allow calculation of at least one PT value. Calculate a K_{fs} value for each PT value using successive Single-PT calculations (see Table A2). Alternative (and more complicated) PT calculation methods (Dual-PT and Multiple-PT analyses) are described in Reynolds (2015).

It should be noted that the borehole radius (a) used in the calculation of K_{fs} from PT (Eqs. 4.3, 4.4, A5) must be replaced with an "effective" radius, a_E [L], if the CHWP outflow tube is left in the hole during the PT measurements. The effective borehole radius is given by:

$$a_E = \sqrt{a^2 - a_O^{\,2}} \quad (7)$$

where a [L] is the actual borehole radius, and a_O [L] is the outside radius of the CHWP outflow tube. The effective radius accounts for reduced borehole volume (due to the presence of the CHWP outflow tube), which in turn causes the borehole ponding depth (H) to fall at a greater rate.

Table A2. Determination of Percolation Test Perc Time (*PT*) and Conversion to Field-Saturated Hydraulic Conductivity (K_{fs}) using successive Single-PT analyses: Example calculations.

The successive Single-PT analysis is given by (Reynolds, 2015):

$$PT_i = \frac{\Delta t_i}{\Delta H_i} = \frac{\overline{C}_i a^2}{K_{fs}\left[2\overline{H}_i^{\,2} + \overline{C}_i a^2 + \left(2\overline{H}_i/\alpha^*\right)\right]} \quad ; i = 1, 2, 3, \ldots, \text{etc.} \tag{A4}$$

where

$$PT_1 = \frac{\Delta t_1}{\Delta H_1} = \frac{t_1 - t_0}{H_0 - H_1}; \quad PT_2 = \frac{\Delta t_2}{\Delta H_2} = \frac{t_2 - t_1}{H_1 - H_2}; \quad PT_3 = \frac{\Delta t_3}{\Delta H_3} = \frac{t_3 - t_2}{H_2 - H_3}; \quad \text{etc.}$$

$$\overline{C}_1 = \left[\frac{\left(\overline{H}_1/a\right)}{Z_1 + Z_2\left(\overline{H}_1/a\right)}\right]^{Z_3}; \quad \overline{C}_2 = \left[\frac{\left(\overline{H}_2/a\right)}{Z_1 + Z_2\left(\overline{H}_2/a\right)}\right]^{Z_3}; \quad \overline{C}_3 = \left[\frac{\left(\overline{H}_3/a\right)}{Z_1 + Z_2\left(\overline{H}_3/a\right)}\right]^{Z_3}; \text{ etc.}$$

$$\overline{H}_1 = \frac{H_0 + H_1}{2}; \qquad \overline{H}_2 = \frac{H_1 + H_2}{2}; \qquad \overline{H}_3 = \frac{H_2 + H_3}{2}; \quad \text{etc.}$$

and *C, a, H,* and α^* are as defined in Table A1.

From field Perc Test measurements: PT_1 = 0.98 min cm^{-1} = 2.49 min in^{-1}
PT_2 = 1.04 min cm^{-1} = 2.67 min in^{-1}
PT_3 = 1.13 min cm^{-1} = 2.87 min in^{-1}

where: a = 0.03 m; α^* = 12 m^{-1}
H_0 = 0.15 m; H_1 = 0.14 m; H_2 = 0.13 m; H_3 = 0.12 m
t_0 = 0 min; t_1 = 0.98 min; t_2 = 2.02 min; t_3 = 3.15 min
$\overline{H}_1$ = 0.145 m; $\overline{H}_2$ = 0.135 m; $\overline{H}_3$ = 0.125 m
$\overline{C}_1$ = 1.6323; $\overline{C}_2$ = 1.5612; $\overline{C}_3$ = 1.4872

Conversion to K_{fs} is given by (Eq. 4.3 in text):

$$K_{fsi} = m_i PT_i^{-1} = \frac{\overline{C}_i a^2}{PT_i\left[2\overline{H}_i^{\,2} + \overline{C}_i a^2 + \left(2\overline{H}_i/\alpha^*\right)\right]} \tag{A5}$$

which yields:
K_{fs1} = 3.69 x 10^{-6} m s^{-1}; K_{fs2} = 3.73 x 10^{-6} m s^{-1}; K_{fs3} = 3.70 x 10^{-6} m s^{-1}